 doi:10.20944/preprints202209.0169.v1

Article

Integration of Sentinel 1 and Sentinel 2 Data for Crop Classification Improvement: Barley and Wheat as an Example

Gaylan R. Faqe Ibrahim [1,2]* Azad Rasul [2] and Haidi Abdullah [3,]

[1] Geography Department, Faculty of Arts, Soran University, Kurdistan Region, Soran, 44008, Iraq; gailan.faqe@soran.edu.iq and azad.rasul@soran.edu.iq
[2] Department of Geography, College of Human Sciences, University of Halabja, Halabja, 46006, Iraq; gailan.faqe"soran.edu.iq
[3] Faculty of Geo-Information Science and Earth Observation (ITC), University of Twente, P.O. Box 217, 7500 AE, Enschede, The Netherlands; abdullah34748@alumni.itc.nl
* Correspondence: gailan.faqe@soran.edu.iq; Tel.: (009647504618417;

Abstract: Observing cultivated crops and other forms of land use is an important environmental and economic concern for agricultural land management and crop classification. Crop categorization offers significant crop management data, ensuring food security, and developing agricultural policies. Remote sensing data, especially publicly available Sentinel 1 and 2 data, has effectively been used in crop mapping and classification in cloudy places because of their high spatial and temporal resolution. This study aimed to improve crop type classification by combining Sentinel-1 (Synthetic Aperture Rader (SAR)) data and the Sentinel-2 Multispectral Instrument (MSI) data. In the study, Random Forest (RF) and Classification and Regression Trees (CART) classier were used to classify grain crops (Barley and Wheat). The classification results based on the combination of Sentinel-2 and Sentinel-1 data indicated an overall accuracy (OA) of 93 % and a kappa coefficient (K) of 0.896 for RF and (89.15%, 0.84) for the CART classifier. It is suggested to employ a mix of radar and optical data to attain the highest level of classification accuracy since doing so improves the likelihood that the details will be observed in comparison to the single-sensor classification technique and yields more accurate results.

Keywords: Synthetic Aperture Rader (SAR); Optical image (Sen-tinel 2); Random Forest (RF); CART; GEE

1. Introduction

It is obvious that agriculture can be considered the "backbone" of human life and has significant control over the economy [1]. Wheat (Triticum ssp.) and barley (Hordeum vulgare L.) are the two most significant temperate cereal crops in terms of economic significance among the roughly 30 types and 360 species that make up the tribe Triticeae (subfamily Pooideae, family Poaceae) [2]. Therefore, the public and private sectors always need to obtain reliable agricultural information, in order to make comprehensive decisions for agricultural policy, provide crops at the lowest cost and guarantee food security [3]. Monitoring agricultural areas are critical to mitigating challenges facing the world such as population growth, increased demand for food and climate change [4], and alterations in consumption habits [3]. Dealing with these challenges requires spatial and temporal information for the distribution of crops, as well as location-based crop classification maps to estimate crop harvest forecasts during the growing season [5]. Crop maps entail detailed temporal and spatial information, where agricultural fields are developed and managed by a diversity of social or policy activities that can have a significant impact on

Preprints (www.preprints.org) | NOT PEER-REVIEWED | Posted: 13 September 2022 doi:10.20944/preprints202209.0169.v1

biochemical, hydrological, climatic, biological, economic and human health cycles. Some local governments use manual labor to implement social policies, identify farm characteristics, and estimate the amount and type of crops harvested in a given area [6], however, new techniques are essential to be used.

Crop classification and obtaining information about farmlands is one of the most important agricultural practices through remote sensing at local and global scale. It is useful for the design and implementation of agricultural policy, crop management and food security[7]. Remote sensing has found widespread use during the last few decades, notably in the field of precision agriculture. The geographical variation that is covered by various crops may be estimated in large part by crop identification and categorization [8]. Field mapping demands a significant amount of time and effort despite, its exceptional precision. The opportunities for field study are severely impacted by the high-mountain vegetation, its restricted availability and shorter vegetation season compared to lowlands. Remote sensing data, which are distinguished by increased objectivity and spatial coverage, are employed more frequently as a result of the quick development of technology [9].

Remote sensing technique is popular and effective to create crop map distribution. It enables rapid and efficient mapping of agricultural land cover, enabling several worldwide cultivated observing applications [10]. Since these data span huge areas at multiple time and spatial resolutions, it is usual practice to use remote sensing data to identify crop kinds. The classification of various crop kinds is based on how those reflectance properties change during the year, therefore the temporal aspect is almost always taken into account [4]. Crop maps have been produced using a multi-spectral and multi-temporal remote sensing data, which has previously demonstrated its capacity to assess vegetation status over different periods [8]. In comparison to conventional ground-based surveys, which are costly and time-consuming, remote sensing-based approaches have been shown to be an efficient method for crop categorization and crop area assessment [11].

Satellite land monitoring offers information about biodiversity, surface characteristics, and spatial differences at a given time, which are very rich sources of information for crop species identification, and can be utilized to monitor them throughout the growth cycle [7]. Aerial imagery is one of the most valuable sources of information for automated land classification and development of various crops grown in different agricultural areas worldwide, which can estimate the area of certain crops, monitor their health and predict their production [12]. The classification and identification of diverse crop categories are based on their variable reflectance properties throughout the year which are constantly taken into account [4]. The classification was performed using a variety of spectral bands from multispectral time series data. Along with time series data, several vegetation indices produced from multispectral images have also been utilized to augment the information and more accurately distinguish areas of vegetation and non-vegetation[8], visible and infrared sensors have been widely used for crop type classification and crop area assessment [13].

Satellite sensors are particularly important because of their excellent spatial resolution, which allows scientists to dramatically reduce the expenses of ongoing monitoring of landscape elements. Sentinel-2 data might be regarded as revolutionary in this situation since in addition to having a short revisit period (five days), it also has the best possible spectral and spatial resolution. Due to the physiognomic changes occurring in the vegetation, the greater number of data gathering allows for the creation of multi-temporal compositions, i.e., images consisting of information collected at various times of the growing season, which may have a discernible effect on the classification outcomes [9]. More recently, the free availability of Sentinel images with high spatial and temporal accuracy has provided sufficient opportunities for agricultural activities [11]. [14] indicated that ((Sentinel-1A, 2A have significant classification capability of crops and proposed the integration of ((Sentinel-1A, 2A) for high accuracy grain classification, which is still rarely being employed [15]. Nevertheless, several studies found that using both optical and radar data together increased mapping accuracy compared to using only one sensor to classify the land cover [16–19].

Supervised classifiers that employ the maximum-likelihood method are the key component of conventional classification. These traditional classifiers were no longer able to comprehend the intricacy of such important data since fine resolution data has recently become more accessible [20]. However, the radiation reflectance in wheat and barley is very similar, so it is necessary to use Sentinel-1 and 2 to make the classification results more accurate. Therefore, the classification methods employed in this study are based on the classification and regression tree (CART) and random forest algorithms (RF). The selection of the classification methods is based on their wide-ranging use in land use categorization.

The SAR data enable to permit the stringent data needs of effective crop monitoring and the appearance of clouds or haze has no impact on SAR data and it can collect data during the day and at night. Furthermore, compared to Sentine-2 wavelengths, microwaves may penetrate plants more thoroughly. Plant water content has a significant impact on SAR signal [21]. SAR data relies on frequency and polarization, it provides a complicated depiction of topography, surface coarseness, soil moisture, and canopy structure, while utilizing optical data, which uses the visible, near-infrared, and short-wave infrared range of the electromagnetic radiation, allows researchers to learn significant details about the water content, leaf pigments, and general health of vegetation [22].

The main aims of this study are to combine optical and SAR data to (1) demonstrate how combining Sentinel-1 and Sentinel-2 increases overall accuracy, (2) to identify crop types classes with high accuracy as a result of combining different sensors, and (3) to evaluate different methods for crop mapping. The output of the research will contribute effectively by adding more knowledge to the field to the ongoing attempt to improve classification approaches and it helps to efficiently classify crop fields.

2. Data and Methodology:

2.1. Study area:

The study site covers the Harir plain of Erbil Province in the north-eastern part of Iraqi Kurdistan, it is 4742.6 ha and located between latitudes 36° 23' 17" N and 36° 40' 05"N and longitudes 44° 8' 1" E and 44° 29' 15"E, and it is approximately (47.3) km far from Erbil city. The study area shares a boundary with Soran district from the north and northeast, Ranyah from the South, Akre in the North West (Figure: 1). The climate of the study site is parallel to that of the Mediterranean region which is characterized by semi-arid climate, according to Köppen classification [23] summers are hot and dry, and winters are cold and rainy. Rainfall is inadequate for the period between October and November, averaging (543) mm annually [24]. According to the classification of soil, the study area consists of (4) types of soil which are a mixture of lithology with limestone, brown soils with medium thickness and deeply covered with lucky dust Stone [25].

 doi:10.20944/preprints202209.0169.v1

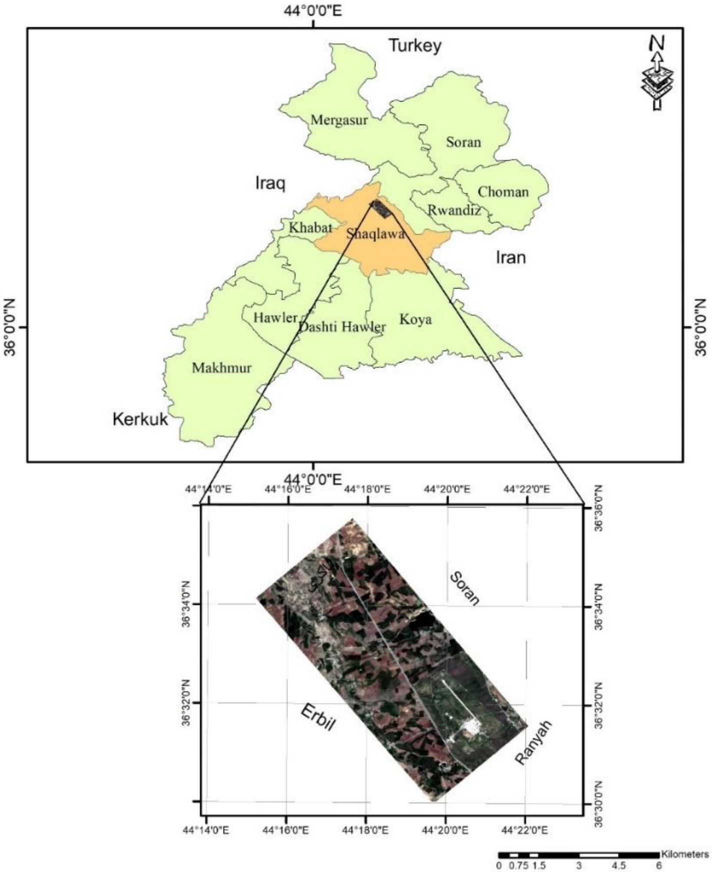

Figure1: illustration of the location of the study area (Harir plain)

2.2. Data source and pre-processing:

The Sentinel-1 and Sentinel-2 satellite programs place a strong premium on land use land cover monitoring, mainly in regions of rapid alteration [15]. In this study, Optical and SAR imagery from the two sensors Sentinel-2 and Sentinel-1 were utilized. The selection of these two sensors is primarily based on their obtainability, as well as the high spatial, spectral, and temporal resolutions they provide. Both Sentinel-1 and Sentinel-2 data were obtained in the GEE platform, taking into account Sentinel-2 product's cloudy coverage of less than 10% and the difference between both images is only two days.

The Sentinel-1 satellite was launched by the European Space Agency (ESA) on April 3, 2014. Sentinel-1 is a two-satellite constellation mission, with 1B scheduled to launch in 2018 [26]. Sentinel-1 is equipped with a C-band in four imaging modes (EW, IW, SM, and WV) with various spatial resolutions (10, 20, 60 m) and coverages an antenna transmits microwave signals to an exact region of the Earth's surface for synthetic aperture radar (SAR) imaging. It is possible to measure the microwave energy reflected to the spacecraft. The radar concept is used to produce SAR images, which uses the time delay of backscattered signals to produce an image. SAR images are appropriate and valuable for evaluating alterations on the Earth's surface caused by the SAR system's operation at all times and in all-weather situations [27].

The present study depends on SAR data Interferometric Wide (IW) Swath mode in dual polarization mode (VV, VH) from 19 April 2022 Table (1). In addition, The SAR data had to be pre-processed after they were acquired in order to draw out useful information for the classification procedure. SAR data is created by the coherent interaction of the emitted microwave with the targets, as opposed to optical images. As a result, it is impacted by the speckle noise, which results from the coherent addition of signals scattered by ground scatters dispersed at random among the pixels. The fluctuation of pixel values around a mean that corresponds to the target's intended backscattering coefficient is referred to as speckle [28]. A SAR image appears visually noisier than an optical one. Speckle is caused by the interference waves reflected from numerous elementary scatters, which appear as grainy noise in SAR images. To reduce radar speckle, a smoothing filter with the function focal mean and a smoothing radius of 50 meters was used. The process of speckle filtering improves image quality by removing speckles [29]. A considerable body of study has been done on modelling and the elimination of speckle [30–32]. Therefore, a speckle noise removal filter is necessary before display and further analysis.

Sentinel-2 is the second data that was used in this study. The polar-orbiting Sun-synchronized Sentinel-2 between the latitudes of 84° North and 56° south, the two satellites have a temporal resolution of 10 days with one satellite and 5 days with two satellites [33]. Different pre-processing techniques were used on Sentinel-2 data. Data from Sentinel-2 were automatically processed. Sentinel-2A is equipped with high-resolution optical equipment with spatial resolutions of (10m, 20m and 60 m), and 13 bands with a wavelength range of 443 nm to 2190 nm. To identify crop types, ten spectral bands in addition to NDVI were employed in this study, including (Blue, Green, Red, Red Edge 1, Red Edge 2, Red Edge 3, NIR, Red Edge 4, SWIR1, and SWIR2. Bands 1 (coastal aerosol), 9 (water vapor), and 10 (SWIR-cirrus) were removed from the analysis since crop type mapping was not relevant to them. Each of the bands of vegetation red-edge (5, 6, 7, 8A), and SWIR (11, 12) was resampled from 20 m to 10 m spatial resolution. In addition, Normalized Difference Vegetation Index (NDVI) was generated in sentinel-2 using bands NIR (8) and red (4). It combined with Sentinel 2 bands to improve the classification technique.

Table 1: Main attributes from the Synthetic Aperture Radar (SAR) dataset Sentinel-1.

Operation	Since April 3, 2014	imaging date	19/04/2022
Orbit hieght	693 km	Swath width	250km
Inclination	98.18	SAR Sub-swaths	3
Wavelength	C-band (3.75-7.5cm)		
Polarization	Dual(VV, VH)	spatial resolution	5*20m (single look
Temporal resolution	6days	pixel Spacing	2.3*17.4 m

2.3. Methodology:

The method utilized in this study consists of four key steps, data collection, pre-possessing, classification and accuracy assessment. Figure 2 illustrates the sequence of the diverse steps just mentioned. Since the first two steps have already been discussed, the third and fourth stages will be discussed in detail in the following section.

2.3.1. Sampling Strategy:

The reference polygons were split into training polygons (70%) and testing polygons (30%), based on crop type and the area of the field. The study separated training and testing polygons to detect how well models performed across different crop types and filed sizes. The polygons used for training were sampled using stratified random sampling with (182) polygons (57883 pixels) for all crop types. This study gathered different random samples according to class sizes, such as wheat (70) polygons (26499 pixels), barley (18) polygon (7281 pixels), uncultivated land (63) polygons (17708 pixels), airport and resident area (33) polygons, (1546 pixels), bareland (16) polygons (1311 pixels), grassland (14) polygons (3538 pixels), random samples. In addition, 30% of samples were used as testing points for validation. Furthermore, (92) polygons, (24786) pixels, were used for testing which is 30% of all samples for all crop types (Table 2). The study employed a random forest and classification and regression trees (CART) classifier. Classified images were exported from GEE to Google Drive and then downloaded.

2.3.2. Image classification:

In this study, Google Earth Engine (GEE) was employed for image classification which is a cutting-edge cloud-based platform for the processing of remote sensing data. Remote Sensing images (Sentinel 1&2) are available in GEE. The choice of an appropriate classification technique is a crucial step to the effective synergetic classification of crop classes, together with the accurate selection and pre-processing of satellite input data. In this study, Random Forest and CART classification were used.

Fgure2: The flowchart for crop type classification using Sentinel-1 and Sentinel-2 data

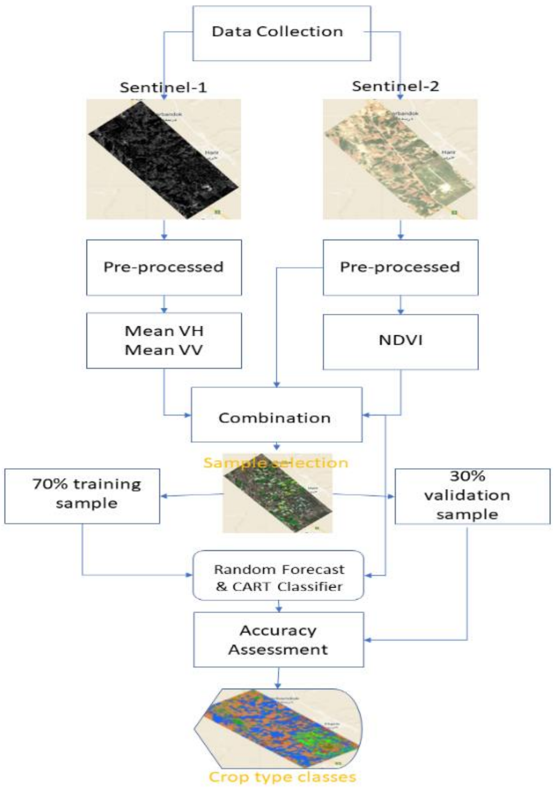

Random Forest Classification:

Preprints (www.preprints.org) | NOT PEER-REVIEWED | Posted: 13 September 2022 doi:10.20944/preprints202209.0169.v1

The decision tree is one of the most widely used methods for identifying patterns or predicting target variables, which splits the input space into parts and gives each sector a response value. Using grouped rules to integrate the predictions of many independent algorithms, Random Forest is a novel way of developing decision trees. Each tree is made by replacing each fixed design with a distinct group of existing patterns. The total number of obtainable methods will be utilized to detect the size of this selected class [34]. The non-parametric RF technique proposed by [35] was used to digitally categorize images into crop types using GEE. These algorithms were selected because of their reliability and precision in classification [36], as well as their continuing excellent performance, ease of parameterization, and robustness [37]. Many studies concentrating on crop type mapping indicated that RF findings are often reliable [38–40].

The RF is a classification algorithm containing several decision trees. Each one is produced from randomly picked training pixels [41]. The RF method is a flexible ensemble learning approach that mixes K binary classification. Each tree is created by implementing a unique learning algorithm into subsets of the input variable sets that were divided using the Gini index as one of the attribute value tests [42,43]. To create a prediction model, the RF classifier just requires the determination of two parameters: the desired number of classification trees (k), and the number of prediction variables (m), which are utilized in each node to create the tree growth [44]. Furthermore, the RF classifier operates effectively with large datasets. Recent research demonstrated that RF can integrate several remote sensing characteristics with categorical land use data to enhance classification performance and to distinguish between forests and other ground covers [45].

Classification and Regression Trees (CART):

CART is a sophisticated method based on a Decision Tree (DT) classifier, which is created from a collection of training data. It is a nonparametric modelling technique that may be used to interpret reactions of a dependent factor using a collection of independent continuous or classified variables [46]. The CART is a binary multivariate statistical method that can process continuous and nominal properties as targets and predictors. No binning is necessary or advised; data are handled in their raw state [47]. [48] showed that the CART classifier was not only precise but also processed a huge quantity of data in a very short amount of time. The benefit of CART is that it is easy to comprehend, visualize, and interpret. CART can handle both classified and numerical data [49]. CART analysis has another advantage which is a mostly automated "machine learning" technique. In other words, the analyst needs none to very minimal input based on the intricacy of the study [50]. The negative part about CART is that it may produce excessively complicated trees that do not generalize the data, a process known as overfitting. Additionally, it has a high degree of sensitivity to the training datasets; a slight change in the training data might lead to a completely different collection of subsets [49].

2.3.3. Accuracy assessment:

The confusion matrix was used to calculate the classification findings' overall accuracy (OA), kappa coefficient, producer's accuracy (PA), and user's accuracy (UA) [15].). A confusion matrix is a sample computation of categorized map and reference data that

 doi:10.20944/preprints202209.0169.v1

has been cross-tabulated. Comparing the images allows for a qualitative assessment of the classification findings while employing statistical tools such as the confusion matrix and the Kappa index allows for a quantitative assessment of the land use land cover classification's accuracy [51]. The overall accuracy (OA) was defined as the percentage of properly classified sampled pixels (Equation 1), while the kappa coefficient is a measure of classification performance that takes into account the chance agreement between the prediction and reference data (equation 2). UA denotes the likelihood that a certain labelled sample will be accurately categorized, while PA denotes the percentage of a given reference class that is correctly classified. This study used 30 percent of the 182 samples using the error matrix of each categorized image, Kappa and overall accuracy were calculated for accuracy assessment (Table 2).

$$OA = \frac{\sum_{i=1}^{k} x_{ii}}{N}, \ldots\ldots\ldots\ldots\ldots\ldots\ldots\ldots\ldots.1$$

Xii = number of diagonal pixels (correctly classified)

N= total number of pixels.

$$K = \frac{A_0 - A_c}{1 - A_c} \ldots\ldots\ldots\ldots\ldots\ldots\ldots\ldots\ldots\ldots 2$$

A_0 The obtained OA or the actual percentage of classified land

A_c Probability of obtaining a correct classification.

Table 2: Description of the training and validation samples

Class name	Training Polygons	Validation Polygons	Training Pixels	Validation Pixels
Wheat	70	30	26499	11327
Barley	18	7	7281	3105
Uncultivated Land	63	27	17708	7691
Airport and Roads	33	14	1546	686
Bareland	16	7	1311	548
Grassland	14	7	3538	1553

3. Results

3.1. Image classification:

The Random Forest and CART classifier were used to produce the crop type map in the study area, the total site of concern is about (4742.6 ha) in Table 3 and Figure 3, and the exact area of the crop types of this study are listed. Table 3 indicates that the wheat area covers the largest area with a total of about 1812.5 hectares and 38.2%, according to Random Forest classification, while the area of the same category with the CART classification is 1741 hectares 36%, followed by wheat, barley, uncultivated and grassland occupying the largest area with 37.6% and 34%, 9.4%, 13.1%, 8.5% and 9.4%, respectively, according to the random forest and card classification respectively, while it was observed

 doi:10.20944/preprints202209.0169.v1

that the bare land, residential land and airport have the lowest area with 3.9%, 4.1 and 2.3%, 2.7%, respectively.

Table 3. Shows the quantity of crop types and other land use classes over the study area

Classes	Area Hectares (RF)	Area % (RF)	Area Hectares (CART)	Area % (CART)
Wheat	1812.5	38.2	1741	36.7
Barley	447.67	9.4	620.48	13.1
Uncultivated land	1783.5	37.6	1610.9	34.0
Airport and Resident area	108.32	2.3	129.66	2.7
Bareland	187.06	3.9	193.93	4.1
Grassland	403.5	8.5	446.58	9.4
Total	4742.6	100.0	4742.6	100.0

Figure 3: crop type map classification obtained from RF and CART classifier

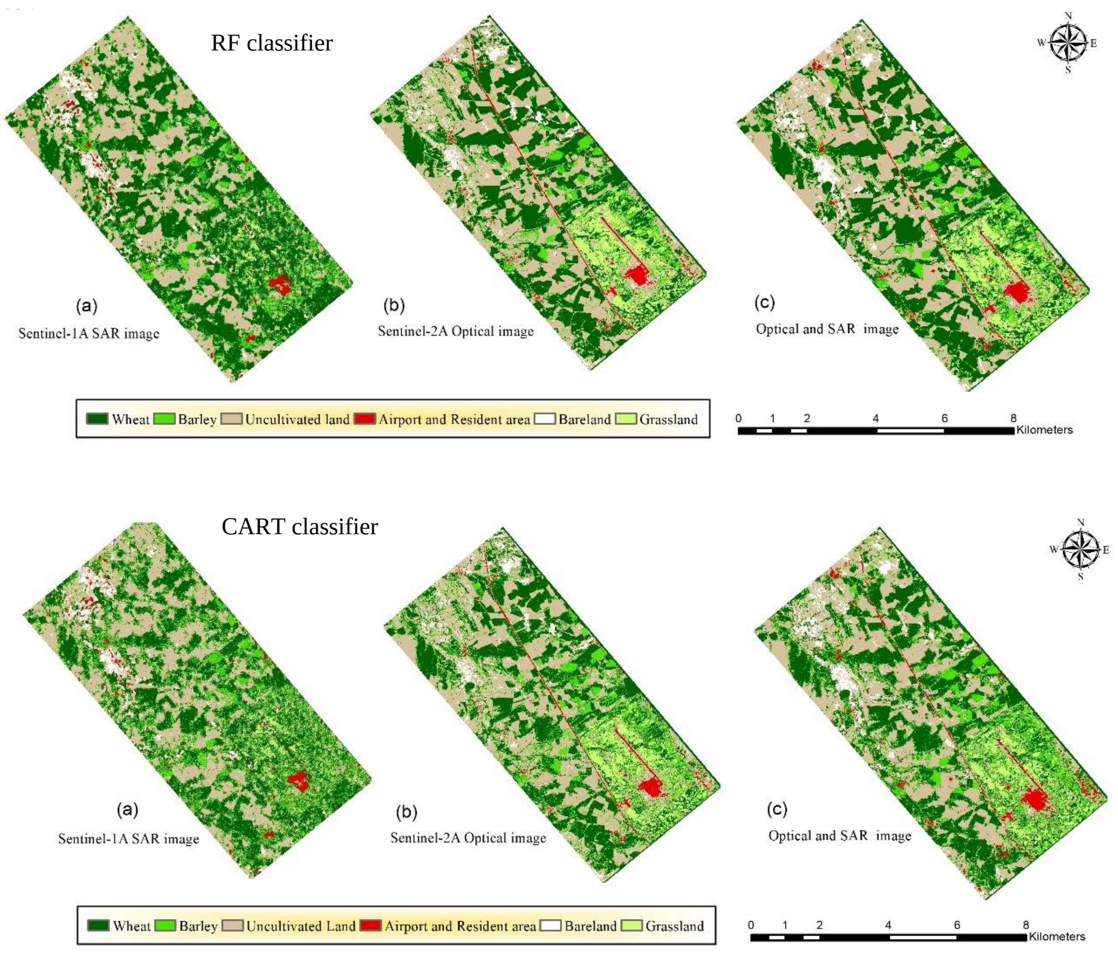

3.2. Accuracy Assessment:

In addition, the classification utilizing the sentinel-1 (SAR) attains an overall accuracy (AO) of 72.91 and 65.04 with Kappa of 0.58 and 0.49 for RF and CART classification, respectively (Table 4). The highest PA that was obtained for both the RF and CART algorithms are for uncultivated land (83% and 81.7%), followed by airport and road (79.3%) for RF classification, then wheat (74.8 and 74.6), bare land (59.5% and 50.8%), barley (38.4% and 27.5%), and grassland (18.4% and 12.6%), respectively. The PA for uncultivated, airport and road, wheat and bare land are quite high. The PA rate for uncultivated is 83.0% because of the total wheat pixels (6616 pixels), 432 pixels are classified as wheat, 470 pixels are classified as barley, 48 pixels are classified as airport roads, 243 pixels are classified as bare land and 161 pixels Classified as Grassland in (RF), while the rate of PA for uncultivated is (81.7%) in (CART) classifier due to in the total wheat pixels (6113 pixels), 473 pixels are classified as barley, 45 pixels are classified as airport roads, 230 pixels are classified as bare land and 170 pixels Classified as Grassland (Table 5). The PA for grassland and barley is less than 35%, which indicates a significant omission error.

Table 4: Confusion matrix of the classification results using the SAR (RF Classifier).

Classes	Wheat	Barley	Uncultivated land	Airport and road	Bareland	Grassland	User's accuracy
Wheat	9977	821	432	50	14	221	86.6
Barley	1672	842	470	17	1	118	27.0
Uncultivated land	359	250	6616	14	95	82	89.2
Airport and road	185	74	48	348	10	8	51.7
Bareland	71	18	243	6	182	5	34.7
Grassland	1067	190	161	4	4	98	6.4
Producer's accuracy	74.8	38.4	83.0	79.3	59.5	18.4	

omission error	
Overall accuracy	72.9140597
Kappa	0.5778655

In addition, the user's accuracies (UA) is highest for uncultivated land (89.2% and 81.4%), followed by wheat (86.6% and 72.8%), airport and road (51.7% and 50.8), bare land (34.7% and 32.6%), barley (27% and 29.8%), and grassland (6.4% and 12.8%) for both (RF and CART) classifiers respectively. The UA rate for uncultivated is 89.2% because 359 pixels are classified as wheat, 250 pixels are classified as barley, 14 pixels are classified as airport roads, 95 pixels are classified as bare land and 82 pixels are classified as Grassland in (RF), while the rate of UA for uncultivated is (81.3%) in (CART) classifier due to 463 pixels being classified as wheat, 472 pixels classified as barley, 47 pixels classified as airport and road, 247 pixels classified as bare land and 170 pixels classified as Grassland (Table 5). The PA for barley, airport and road, and bareland are less than 60%, which indicates a significant omission error.

Table 5: Confusion matrix of the classification results using the SAR (CART Classifier)

Preprints (www.preprints.org) | NOT PEER-REVIEWED | Posted: 13 September 2022 doi:10.20944/preprints202209.0169.v1

Classes	Wheat	Barley	Uncultivated land	Airport and road	Bareland	Grassland	User's accuracy
Wheat	8273	1502	473	177	81	860	72.78
Barley	1282	894	450	71	30	268	29.84
Uncultivated land	463	472	6113	47	247	170	81.37
Airport and road	180	60	45	333	16	21	50.83
Bareland	72	24	230	21	175	15	32.58
Grassland	814	302	170	7	18	192	12.58
Producer's accuracy	74.63	27.47	81.71	50.76	30.86	12.58	

Omission error	
Overall accuracy	65.04395962
Kappa	0.486524667

The Sentinel-2 categorization image noted low omission and commission errors as well as higher overall and Kappa as compared with sentinel-1. The overall accuracy is 88.978 and 85.081 and Kappa is 0.8299 and 0.7808 for RF and CART classification (Table 6). According to the aforementioned findings, Sentinel-1 SAR data determine land cover types less accurately than Sentinel-2 data at the same spatial resolution. The PA accuracy was high for the airport and roads (97.57% and 96.97%), uncultivated land 92.12% and 91, 01%), wheat 90.1% and 89, 55%, bareland 88.05% and 77.87%, but it decreased for the classes of barley and grassland (less than 70%). The UA for all classes that are quite higher exclude barley in the RF algorithm. The obtained UA is highest for airport and road (98.02% and 95.96%), then uncultivated land (9515% and 91.41%), wheat (95.22% and 89.53%), bare land (83.81% and 78.01%), grassland (73.95% and 66.79%) for both (RF and CART) classifier, respectively. The lowest user accuracy showed in barley (41.15% and 61.91%) for both algorithms, respectively. When the classification results of Sentinel-1 are compared with those of Sentinel-2, it is observed that the overall accuracy and Kappa of Sentinel-2 is much higher than that of Sentinel-1 ،as well as, the classification accuracy of Sentinel-2 classes is also much better than that of Sentinel-1.

Table 6: Confusion matrix of the classification results using the Optical Sentinel-2 (RF Classifier)

Classes	Wheat	Barley	Uncultivated land	Airport and road	Bareland	Grassland	User's accuracy
Wheat	10761	251	165	6	5	113	95.22
Barley	886	879	278	0	11	82	41.15
Uncultivated land	98	126	7356	2	38	70	95.65
Airport and road	0	0	9	644	4	0	98.02
Bareland	0	3	73	8	435	0	83.81
Grassland	198	96	104	0	1	1133	73.95
Producer's accuracy	90.10	64.87	92.12	97.57	88.05	81.04	

Omission error	
Overall accuracy	65.04395962
Kappa	0.486524667

 doi:10.20944/preprints202209.0169.v1

Table 7: Confusion matrix of the classification results using the Optical Sentinel-2 (CART Classifier)

Classes	Wheat	Barley	Uncultivated land	Airport and road	Bareland	Grassland	User's accuracy
Wheat	10226	811	155	3	17	209	89.53
Barley	768	1980	284	0	14	152	61.91
Uncultivated land	197	257	6908	5	84	106	91.41
Airport and road	2	0	14	642	10	1	95.96
Bareland	5	6	98	12	447	5	78.01
Grassland	221	152	131	0	2	1018	66.79
Producer's accuracy	89.55	61.75	91.01	96.97	77.87	68.27	

Omission error	
Overall accuracy	85.08138882
Kappa	0.780739147

3.3. Improvement Accuracy of Classification

This study also attempted to improve the pixel-level classification results by combining Sentinel-1 SAR data and Sentinel-2 (optical) data. Two Sentinel-1 bands were combined with Sentinel-2 multi-spectrum image bands. The RF and CART classifiers were used to process the integration of SAR data and optical data. It is clear that the Sentinel-1 and Sentinel-2 images together formed a more accurate product. Overall map accuracy for combined Sentinel-1 and Sentinel-2 in the study area were 93.044% and 89.153 of OA and 0.896 and 0.8915 of Kappa, respectively, for both RF and CART classifiers (Table 8), while the Sentinel-1 image alone produced the lowest results of all the analyses (72.91 and 65.04% of OA and 0.58 and 049 of Kappa). When combined optical and SAR Sentinel results compared to classification maps obtained from Sentinel-1 and Sentinel-2, these crop type maps have greater overall map accuracy. All classes improved their accuracy when compared to Sentinel-1 or Sentinel-2 classification separately. These improved class accuracies resulted in fewer errors of both PA and UA, especially in the wheat, barley, bare land and grassland class. The highest PA is obtained for uncultivated land and airport and road (98.27% and 95.34%), then by airport and road (97.34% and 95.91%), wheat (96.85% and 91.92%), bare land (89.15% and 88.5%), grassland (80.22% and 73.34%), and barley (72.1% and 70.43%) for both (RF and CART) classifier, respectively. These increased class accuracies resulted in a lower error of UA and PA, especially, in the airport and roads (Table 8 and 9).

 doi:10.20944/preprints202209.0169.v1

Table 8: Confusion matrix of the classification results using the SAR and Sentinel-2 (RF Classifier)

	Wheat	Barley	Uncultivated land	Airport and road	Bareland	Grassland	User's accuracy
Wheat	11039	186	66	5	1	100	96.85
Barley	688	2210	104	0	0	63	72.1
Uncultivated land	57	43	7444	0	13	18	98.27
Airport and road	0	1	13	659	4	0	97.34
Bareland	0	0	50	8	477	0	89.15
Grassland	194	74	36	0	0	1233	80.22
Producer's accuracy	92.16	87.90	96.51	98.06	96.36	87.19	

Omission error	
Overall accuracy	93.0444606
Kappa	0.89602126

Table 9: Confusion matrix of the classification results using the SAR and Sentinel-2 (CART Classifier)

	Wheat	Barley	Uncultivated land	Airport and road	Bareland	Grassland	User's accuracy
Wheat	11039	186	66	5	1	100	91.92
Barley	688	2210	104	0	0	63	70.43
Uncultivated land	57	43	7444	0	13	18	95.34
Airport and road	0	1	13	659	4	0	95.91
Bareland	0	0	50	8	477	0	88.5
Grassland	194	74	36	0	0	1233	73.34
Producer's accuracy	91.39	71.21	95.46	97.05	86.45	74.63	

omission error	
Overall accuracy	89.15356711
Kappa	0.840511816

4. Disscusion:

4.1. Sentinel-1 images:

The classification applied to the Sentinel-1 image demonstrates that the Sentinel-1 SAR data can discriminate between different crop types. A number of conditions affect the backscattering of different surface covers. The ability of the microwave to detect surface roughness aids in classifying different types of cop types. Figure (4) presents the analysis of discrete classes by means of polarization (VV, VH) having the highest mean values in airport and roads, while Grassland has the lowest mean values.

Polarization VH is weaker for all six classes compared to VV polarization. In the boxplot will notice that VV and VH bands are much more suitable for separating wheat and uncultivated land, grassland and bareland, which have a very slight ability to separate wheat and barley due to their backscatters being very similar. The overall accuracy for wheat and barley is 86.6% and 27%, therefore, using Sentinel-1 solely is not able to separate wheat and barley properly (Table 4). The results show that the backscatter of wheat and barley are very similar. When Sentinel-1 is used alone, wheat and barley have nearly identical backscatter information.

Figure 4. Box plot that represents the backscatter coefficient values land cover classes

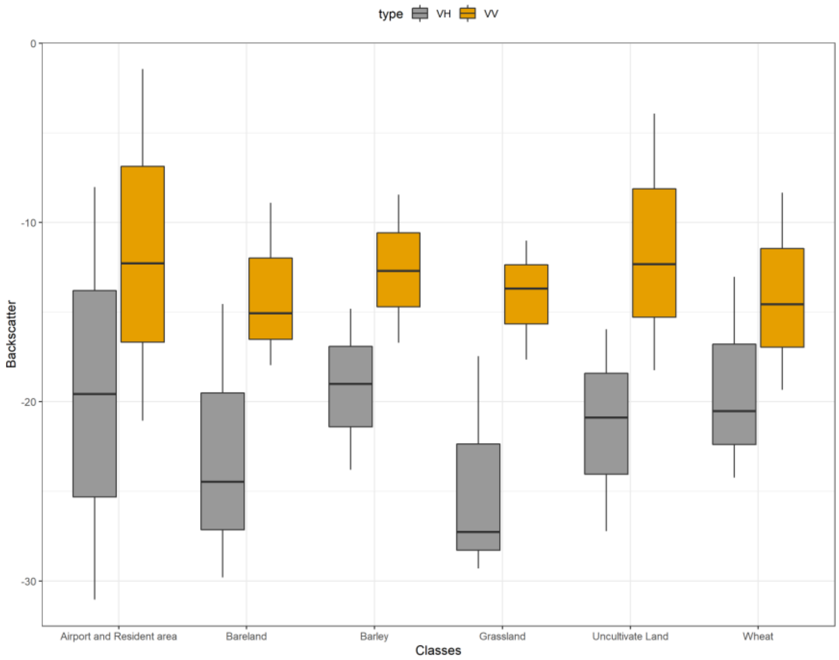

4.2. Spectral reflectance value of Sentinel-2 bands:

The study also can observe that some classes tend to overlap when their spectral responses are relatively comparable in different wavelengths for the bands investigated in the study of variation by the spectral response (surface reflectance) of each class. The best situation to observe for separating classes is by using the green band to separate wheat, bareland, and almost all classes. Red wavelength is also suitable for separating wheat, uncultivated land, airport, grassland, and barley, while near-red, and Red Edge are largely similar in terms of wheat, barley, and grassland.

Figure 5. Wavelengths analysis by crop type class of Sentinel-2 bands

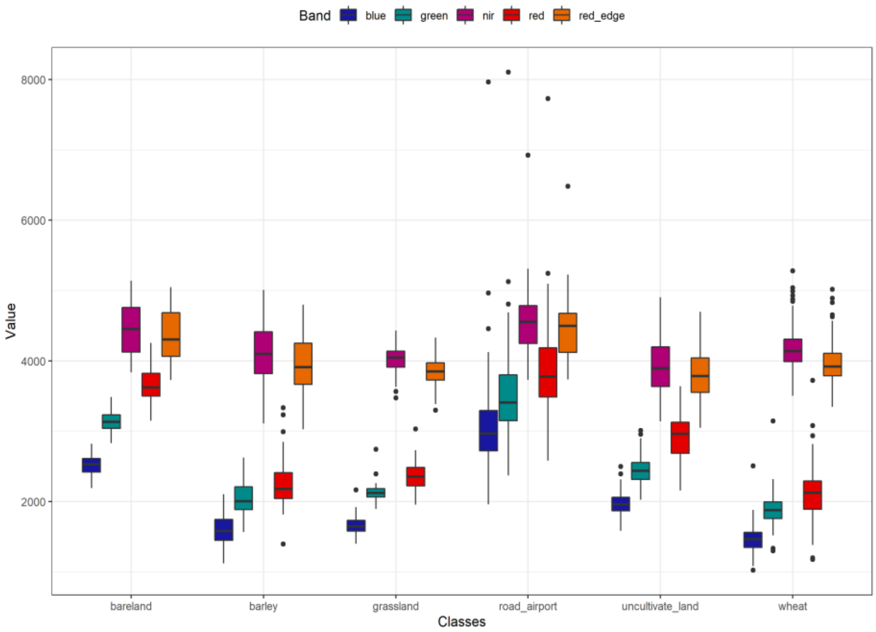

 doi:10.20944/preprints202209.0169.v1

4.3. Crop Classification:

For the protection and management of cereal crops, agricultural land has to be monitored regularly. Additionally, the information on crop types can be utilized to assess crop acreage and yield which crops are crucial for food security. The study investigated the capability of the two widely accessible Sentinel-1 and Sentinel-2, to detect six crucial classes (wheat, barley, uncultivated land, airport and road, bare land, and grassland) across the study area. The RF and CART methods mentioned in previous studies are the two best classification methods, due to their high classification accuracy (Akar & Gungor, 2012; Bayas et al., 2022; Delalay et al., 2019; Firas Mohammed Ali1 et al., 2015; Kaszta et al., 2016). Since these two types of algorithms are the best, this study used both algorithms for Sentinel-1 and Sentinel-2. The study confirmed that the application of optical data and radar data is commonly recognized as a means to improve RF [16,17,19] and CART classification [46,58]. The aforementioned findings demonstrate that the RF is more precise than the CART method.

4.4. Improvement of Crop Classification

These results show that the data derived from the SAR image did not have a significant impact on the classification, whereas the optical product data improved the classification when compared with the result of sentinel-1 (Tables 4 and 5). The OA of sentinel-1A is 72.91% and 65.04%, as well as, the OA for sentinel-2 is 89.97% and 85.08%, this is consistent with the results of [16–18]. The study was able to accurately map crop type, especially when employing both sensors. The best accuracy was recorded for the uncultivated land, airport and residential area and wheat, while the lowest accuracy was recorded for barley, and these tendencies persisted generally across sensor combinations. As noted, the combination of Sentinel-1 and Sentinel-2 images improved the overall accuracy of cereal crop classification for both methods (RF, CART), when compared to the results obtained using only optical or radar single sensitivity. It has an overall accuracy based on Sentinel-1 data (72.91% and 65.043%), while Sentinel-2 data is better than Sentinel-1 radar data with an overall accuracy of 88.97% and 85.081%, respectively. When utilizing the RF method for optical and Radar data, 186 pixels of the wheat are categorized as barley, 66 pixels as uncultivated land, 5 pixels as an airport and road, 1 pixel as bare land, and 100 pixels as grassland. As a result, when the RF algorithm is applied, the PA for the wheat region is 92.16% and the UA is 96.85%, whereas the PA for wheat is 91.39 and the UA is 91.92 when the CART algorithm is applied.

In addition, combining Sentinel-1 and Sentinel-2 images and the addition of Sentinel-2 NDVI layer increased the overall accuracy and Kappa coefficient of classification. The overall accuracy for (RF) was (93%) and Kappa coefficient (0.89) while (89.15%) overall and (0.84) Kappa coefficient for (CART classifier), which are consistent with other findings in different geographical areas that rely on combining optical and radar data, despite increased visit times and enhanced spatial resolutions of Sentinel systems, which helps to make it more versatile and attractive. The study concluded that a combination of Sentinel-2 MSI, Sentinel-1 bands, and NDVI provides a workable alternative for routine crop categorization and monitoring.

 doi:10.20944/preprints202209.0169.v1

4.5. Limitation of the classification

If the classification results of the algorithms are observed, good results are obtained, however, several misclassifications are seen when classifying classes, when classifying wheat, 821 pixels are classified as barley, 432 pixels as uncultivated land, and 221 pixels as grassland Barley is characterized by a large amount of wheat, and a large part of the area of Grassland is located within the airport area. Currently, this area has become a protected area due to security reasons, but in previous years this area was used for wheat and barley the remaining area is grown annually with grassland, so about 221 pixels are classified as wheat. On the other hand, the uncultivated area covers a large part of the study area, which is due to several reasons, one of which is that the government has not provided any financial support and agricultural supplies to farmers in recent years. Also, the Kurdistan Region Government and the central government have been very negligent in selling their grain and paying them. Despite these factors, the drought in recent years has also affected this situation. These factors have caused many farmers to leave their land.

5. Conclusion:

The need to provide population diversity is important as a result of the world's population growth. Identifying the level of consumption and the paths to acquisition is one of the key issues in future planning. In addition, meeting the demands of the farmed crops in terms of fertilizer, water, and early anomaly identification is crucial. New technologies, such as remote sensing and the use of satellite images have essentially resolved these concerns. This study used RF and CART classifiers to crop type classification using fusing sentinel-1 with sentinel-2, which demonstrated that the classification accuracy of the random forest algorithm is much better than that of the CART algorithm by integrating the SAR and Optical data. The outcomes suggest that the classification using the RF classifier gains the highest OA (89.15) and CART (0.8405) classifier. Sentinel-1 SAR data are also employed for discrimination of six land covers which is OA of (72) and (65) with Kappa of (0.5778) and (486524). The classification based on sentinel-1 SAR data produces a lower OA when compared to the classification using sentinel-2. The result also indicated that the accuracy of classification employed only optical characteristics performed better than using simply SAR features. Therefore, this study suggests that the method of this study can be transferred to other areas.

Author contributions: Conceptualization, Gaylan R. Faqe Ibrahim; Formal analysis, Gaylan R. Faqe Ibrahim; Investigation, Gaylan R. Faqe Ibrahim; Methodology, Gaylan R. Faqe Ibrahim; Software, Gaylan R. Faqe Ibrahim; Supervision, Azad Rasul; Validation, Gaylan R. Faqe Ibrahim; Visualization, Azad Rasul; Writing – original draft, Gaylan R. Faqe Ibrahim; Writing – review & editing, Gaylan R. Faqe Ibrahim, Azad Rasul and Haidi Abdullah

Funding: This research received no external funding.

Conflicts of Interest: The authors declare no conflict of interest.

Availability of data and material: Used data available at Google Earth Engine.

References

1. Ennouri, K.; Kallel, A. Remote Sensing: An Advanced Technique for Crop Condition Assessment. *Mathematical Problems in Engineering* **2019**, *2019*, e9404565, doi:10.1155/2019/9404565.
2. Schnurbusch, T. Wheat and Barley Biology: Towards New Frontiers. *Journal of Integrative Plant Biology* **2019**, *61*, 198–203, doi:10.1111/jipb.12782.
3. Lira Melo de Oliveira Santos, C.; Augusto Camargo Lamparelli, R.; Kelly Dantas Araújo Figueiredo, G.; Dupuy, S.; Boury, J.; Luciano, A.C. dos S.; Torres, R. da S.; le Maire, G. Classification of Crops, Pastures, and Tree Plantations along the Season with Multi-Sensor Image Time Series in a Subtropical Agricultural Region. *Remote Sensing* **2019**, *11*, 334, doi:10.3390/rs11030334.
4. Heupel, K.; Spengler, D.; Itzerott, S. A Progressive Crop-Type Classification Using Multitemporal Remote Sensing Data and Phenological Information. *PFG* **2018**, *86*, 53–69, doi:10.1007/s41064-018-0050-7.
5. Hütt, C.; Waldhoff, G. Multi-Data Approach for Crop Classification Using Multitemporal, Dual-Polarimetric TerraSAR-X Data, and Official Geodata. *European Journal of Remote Sensing* **2018**, *51*, 62–74, doi:10.1080/22797254.2017.1401909.
6. Kobayashi, N.; Tani, H.; Wang, X.; Sonobe, R. Crop Classification Using Spectral Indices Derived from Sentinel-2A Imagery. *Journal of Information and Telecommunication* **2020**, *4*, 67–90, doi:10.1080/24751839.2019.1694765.
7. Arias, M.; Campo-Bescós, M.Á.; Álvarez-Mozos, J. Crop Classification Based on Temporal Signatures of Sentinel-1 Observations over Navarre Province, Spain. *Remote Sensing* **2020**, *12*, 278, doi:10.3390/rs12020278.
8. Khaliq, A.; Peroni, L.; Chiaberge, M. Land Cover and Crop Classification Using Multitemporal Sentinel-2 Images Based on Crops Phenological Cycle. In Proceedings of the 2018 IEEE Workshop on Environmental, Energy, and Structural Monitoring Systems (EESMS); June 2018; pp. 1–5.
9. Wakulińska, M.; Marcinkowska-Ochtyra, A. Multi-Temporal Sentinel-2 Data in Classification of Mountain Vegetation. *Remote Sensing* **2020**, *12*, 2696, doi:10.3390/rs12172696.
10. Remelgado, R.; Zaitov, S.; Kenjabaev, S.; Stulina, G.; Sultanov, M.; Ibrakhimov, M.; Akhmedov, M.; Dukhovny, V.; Conrad, C. A Crop Type Dataset for Consistent Land Cover Classification in Central Asia. *Sci Data* **2020**, *7*, 250, doi:10.1038/s41597-020-00591-2.
11. Baidar, T. Rice Crop Classification and Yield Estimation Using Multi-Temporal Sentinel-2 Data: A Case Study of Terai Districts of Nepal. **2020**.
12. Crnojević, V.; Lugonja, P.; Brkljač, B.N.; Brunet, B. Classification of Small Agricultural Fields Using Combined Landsat-8 and RapidEye Imagery: Case Study of Northern Serbia. *JARS* **2014**, *8*, 083512, doi:10.1117/1.JRS.8.083512.
13. McNairn, H.; Ellis, J.; Van Der Sanden, J.J.; Hirose, T.; Brown, R.J. Providing Crop Information Using RADARSAT-1 and Satellite Optical Imagery. *International Journal of Remote Sensing* **2002**, *23*, 851–870, doi:10.1080/01431160110070753.
14. Sonobe, R.; Yamaya, Y.; Tani, H.; Wang, X.; Kobayashi, N.; Mochizuki, K. Assessing the Suitability of Data from Sentinel-1A and 2A for Crop Classification. *GIScience & Remote Sensing* **2017**, *54*, 918–938, doi:10.1080/15481603.2017.1351149.
15. Steinhausen, M.J.; Wagner, P.D.; Narasimhan, B.; Waske, B. Combining Sentinel-1 and Sentinel-2 Data for Improved Land Use and Land Cover Mapping of Monsoon Regions. *International Journal of Applied Earth Observation and Geoinformation* **2018**, *73*, 595–604, doi:10.1016/j.jag.2018.08.011.
16. De Luca, G.; M. N. Silva, J.; Di Fazio, S.; Modica, G. Integrated Use of Sentinel-1 and Sentinel-2 Data and Open-Source Machine Learning Algorithms for Land Cover Mapping in a Mediterranean Region. *European Journal of Remote Sensing* **2022**, *55*, 52–70, doi:10.1080/22797254.2021.2018667.

17. Manakos, I.; Kordelas, G.A.; Marini, K. Fusion of Sentinel-1 Data with Sentinel-2 Products to Overcome Non-Favourable Atmospheric Conditions for the Delineation of Inundation Maps. *European Journal of Remote Sensing* **2020**, *53*, 53–66, doi:10.1080/22797254.2019.1596757.
18. Rao, P.; Zhou, W.; Bhattarai, N.; Srivastava, A.K.; Singh, B.; Poonia, S.; Lobell, D.B.; Jain, M. Using Sentinel-1, Sentinel-2, and Planet Imagery to Map Crop Type of Smallholder Farms. *Remote Sensing* **2021**, *13*, 1870, doi:10.3390/rs13101870.
19. Tavares, P.A.; Beltrão, N.E.S.; Guimarães, U.S.; Teodoro, A.C. Integration of Sentinel-1 and Sentinel-2 for Classification and LULC Mapping in the Urban Area of Belém, Eastern Brazilian Amazon. *Sensors* **2019**, *19*, 1140, doi:10.3390/s19051140.
20. Palchowdhuri, Y.; Valcarce-Diñeiro, R.; King, P.; Sanabria-Soto, M. Classification of Multi-Temporal Spectral Indices for Crop Type Mapping: A Case Study in Coalville, UK. *The Journal of Agricultural Science* **2018**, *156*, 24–36, doi:10.1017/S0021859617000879.
21. Beriaux, E.; Jago, A.; Lucau-Danila, C.; Planchon, V.; Defourny, P. Sentinel-1 Time Series for Crop Identification in the Framework of the Future CAP Monitoring. *Remote Sensing* **2021**, *13*, 2785, doi:10.3390/rs13142785.
22. Orynbaikyzy, A.; Gessner, U.; Mack, B.; Conrad, C. Crop Type Classification Using Fusion of Sentinel-1 and Sentinel-2 Data: Assessing the Impact of Feature Selection, Optical Data Availability, and Parcel Sizes on the Accuracies. *Remote Sensing* **2020**, *12*, 2779, doi:10.3390/rs12172779.
23. Koeppe, C.E. *Weather and Climate [by] Clarence E. Koeppe [and] George C. De Long.*; McGraw-Hill: New York, 1958;
24. Hussein, S.O.; Kovács, F.; Tobak, Z. Spatiotemporal Assessment of Vegetation Indices and Land Cover for Erbil City and Its Surrounding Using Modis Imageries. *Journal of Environmental Geography* **2017**, *10*, 31–39, doi:10.1515/jengeo-2017-0004.
25. Buringh, P. *Soils and Soil Conditions in Iraq*; 1960;
26. Li, X. The First Sentinel-1 SAR Image of a Typhoon. *Acta Oceanol. Sin.* **2015**, *34*, 1–2, doi:10.1007/s13131-015-0589-8.
27. Moumni, A.; Lahrouni, A. Machine Learning-Based Classification for Crop-Type Mapping Using the Fusion of High-Resolution Satellite Imagery in a Semiarid Area. *Scientifica* **2021**, *2021*, e8810279, doi:10.1155/2021/8810279.
28. Mahdavi, S.; Salehi, B.; Moloney, C.; Huang, W.; Brisco, B. Speckle Filtering of Synthetic Aperture Radar Images Using Filters with Object-Size-Adapted Windows. *International Journal of Digital Earth* **2018**, *11*, 703–729, doi:10.1080/17538947.2017.1351582.
29. Filipponi, F. Sentinel-1 GRD Preprocessing Workflow.; June 4 2019; Vol. 18, p. 6201.
30. Ashok, H.G.; Patil, D.R. Survey on Change Detection in SAR Images. *IJCA Proceedings on National Conference on Emerging Trends in Computer Technology* **2014**, *NCETCT*, 4–7.
31. Touzi, R. A Review of Speckle Filtering in the Context of Estimation Theory. *IEEE Transactions on Geoscience and Remote Sensing* **2002**, *40*, 2392–2404, doi:10.1109/TGRS.2002.803727.
32. Yuan, J.; Lv, X.; Li, R. A Speckle Filtering Method Based on Hypothesis Testing for Time-Series SAR Images. *Remote Sensing* **2018**, *10*, 1383, doi:10.3390/rs10091383.
33. ESA Sentinel-2 User Handbook - Sentinel Online Available online: https://sentinels.copernicus.eu/web/sentinel/user-guides/document-library/-/asset_publisher/xlslt4309D5h/content/sentinel-2-user-handbook (accessed on 15 August 2022).
34. Felegari, S.; Sharifi, A.; Moravej, K.; Amin, M.; Golchin, A.; Muzirafuti, A.; Tariq, A.; Zhao, N. Integration of Sentinel 1 and Sentinel 2 Satellite Images for Crop Mapping. *Applied Sciences* **2021**, *11*, 10104, doi:10.3390/app112110104.

35. Breiman, L. Random Forests | SpringerLink Available online: https://link.springer.com/article/10.1023/a:1010933404324 (accessed on 19 August 2022).
36. Denize, J.; Hubert-Moy, L.; Betbeder, J.; Corgne, S.; Baudry, J.; Pottier, E. Evaluation of Using Sentinel-1 and -2 Time-Series to Identify Winter Land Use in Agricultural Landscapes. *Remote Sensing* **2019**, *11*, 37, doi:10.3390/rs11010037.
37. Belgiu, M.; Drăguţ, L. Random Forest in Remote Sensing: A Review of Applications and Future Directions. *ISPRS Journal of Photogrammetry and Remote Sensing* **2016**, *114*, 24–31, doi:10.1016/j.isprsjprs.2016.01.011.
38. Balzter, H.; Cole, B.; Thiel, C.; Schmullius, C. Mapping CORINE Land Cover from Sentinel-1A SAR and SRTM Digital Elevation Model Data Using Random Forests. *Remote Sensing* **2015**, *7*, 14876–14898, doi:10.3390/rs71114876.
39. Inglada, J.; Arias, M.; Tardy, B.; Hagolle, O.; Valero, S.; Morin, D.; Dedieu, G.; Sepulcre, G.; Bontemps, S.; Defourny, P.; et al. Assessment of an Operational System for Crop Type Map Production Using High Temporal and Spatial Resolution Satellite Optical Imagery. *Remote Sensing* **2015**, *7*, 12356–12379, doi:10.3390/rs70912356.
40. Onojeghuo, A.O.; Blackburn, G.A.; Wang, Q.; Atkinson, P.M.; Kindred, D.; Miao, Y. Mapping Paddy Rice Fields by Applying Machine Learning Algorithms to Multi-Temporal Sentinel-1A and Landsat Data. *International Journal of Remote Sensing* **2018**, *39*, 1042–1067, doi:10.1080/01431161.2017.1395969.
41. Nguyen, T.T.H.; Chau, T.N.Q.; Pham, T.A.; Tran, T.X.P.; Phan, T.H.; Pham, T.M.T. Mapping Land Use/Land Cover Using a Combination of Radar Sentinel-1A and Sentinel-2A Optical Images. *IOP Conf. Ser.: Earth Environ. Sci.* **2021**, *652*, 012021, doi:10.1088/1755-1315/652/1/012021.
42. Akbari, E.; Darvishi Boloorani, A.; Neysani Samany, N.; Hamzeh, S.; Soufizadeh, S.; Pignatti, S. Crop Mapping Using Random Forest and Particle Swarm Optimization Based on Multi-Temporal Sentinel-2. *Remote Sensing* **2020**, *12*, 1449, doi:10.3390/rs12091449.
43. Pelletier, C.; Valero, S.; Inglada, J.; Champion, N.; Dedieu, G. Assessing the Robustness of Random Forests to Map Land Cover with High Resolution Satellite Image Time Series over Large Areas. *Remote Sensing of Environment* **2016**, *187*, 156–168, doi:10.1016/j.rse.2016.10.010.
44. Rodriguez-Galiano, V.F.; Ghimire, B.; Rogan, J.; Chica-Olmo, M.; Rigol-Sanchez, J.P. An Assessment of the Effectiveness of a Random Forest Classifier for Land-Cover Classification. *ISPRS Journal of Photogrammetry and Remote Sensing* **2012**, *67*, 93–104, doi:10.1016/j.isprsjprs.2011.11.002.
45. Tatsumi, K.; Yamashiki, Y.; Canales Torres, M.A.; Taipe, C.L.R. Crop Classification of Upland Fields Using Random Forest of Time-Series Landsat 7 ETM+ Data. *Computers and Electronics in Agriculture* **2015**, *115*, 171–179, doi:10.1016/j.compag.2015.05.001.
46. Zheng, H.; Chen, L.; Han, X.; Zhao, X.; Ma, Y. Classification and Regression Tree (CART) for Analysis of Soybean Yield Variability among Fields in Northeast China: The Importance of Phosphorus Application Rates under Drought Conditions. *Agriculture, Ecosystems & Environment* **2009**, *132*, 98–105, doi:10.1016/j.agee.2009.03.004.
47. Steinberg, D. Chapter 10 CART: Classification and Regression Trees. **2009**.
48. Hartfield, K.A.; Marsh, S.E.; Kirk, C.D.; Carrière, Y. Contemporary and Historical Classification of Crop Types in Arizona. *International Journal of Remote Sensing* **2013**, *34*, 6024–6036, doi:10.1080/01431161.2013.793861.
49. Ray, S. EXPLORING MACHINE LEARNING CLASSIFICATION ALGORITHMS FOR CROP CLASSIFICATION USING SENTINEL 2 DATA. *ISPRS - International Archives of the Photogrammetry, Remote Sensing and Spatial Information Sciences* **2019**, *XLII-3/W6*, 573–578, doi:10.5194/isprs-archives-XLII-3-W6-573-2019.
50. Lewis, R. An Introduction to Classification and Regression Tree (CART) Analysis. **2000**.

51. Moumni, A.; Lahrouni, A. Machine Learning-Based Classification for Crop-Type Mapping Using the Fusion of High-Resolution Satellite Imagery in a Semiarid Area. *Scientifica (Cairo)* **2021**, *2021*, 8810279, doi:10.1155/2021/8810279.
52. Akar, Ö.; Gungor, O. Rastgele Orman Algoritması Kullanılarak Çok Bantlı Görüntülerin Sınıflandırılması. *Journal of Geodesy and Geoinformation* **2012**, *1*, 139–146, doi:10.9733/jgg.241212.1t.
53. Bayas, S.; Sawant, S.; Dhondge, I.; Kankal, P.; Joshi, A. Land Use Land Cover Classification Using Different ML Algorithms on Sentinel-2 Imagery. In Proceedings of the Advanced Machine Intelligence and Signal Processing; Gupta, D., Sambyo, K., Prasad, M., Agarwal, S., Eds.; Springer Nature: Singapore, 2022; pp. 761–777.
54. Delalay, M.; Tiwari, V.; Ziegler, A.; Gopal, V.; Passy, P. Land-Use and Land-Cover Classification Using Sentinel-2 Data and Machine-Learning Algorithms: Operational Method and Its Implementation for a Mountainous Area of Nepal. *Journal of Applied Remote Sensing* **2019**, *13*, 1, doi:10.1117/1.JRS.13.014530.
55. Firas Mohammed Ali1; , Dr. Prof. El-Bahlul Emhemed Fgee2; , Dr.Prof.Zakaria Suliman Zubi PREDICTING PERFORMANCE OF CLASSIFICATION ALGORITHMS. **2015**, *6*, 19–28.
56. Kaszta, Ż.; Van De Kerchove, R.; Ramoelo, A.; Cho, M.A.; Madonsela, S.; Mathieu, R.; Wolff, E. Seasonal Separation of African Savanna Components Using Worldview-2 Imagery: A Comparison of Pixel- and Object-Based Approaches and Selected Classification Algorithms. *Remote Sensing* **2016**, *8*, 763, doi:10.3390/rs8090763.
57. Kumar, P.S.; Pranavi, S. Performance Analysis of Machine Learning Algorithms on Diabetes Dataset Using Big Data Analytics. In Proceedings of the 2017 International Conference on Infocom Technologies and Unmanned Systems (Trends and Future Directions) (ICTUS); December 2017; pp. 508–513.
58. P, T.; Sathiaseelan, J. A Comparative Study of SVM, RF and CART Algorithms for Image 2016.
59. Qu, L.; Chen, Z.; Li, M. CART-RF Classification with Multifilter for Monitoring Land Use Changes Based on MODIS Time-Series Data: A Case Study from Jiangsu Province, China. *Sustainability* **2019**, *11*, 5657, doi:10.3390/su11205657.
60. Saranya, T.; Sridevi, S.; Deisy, C.; Chung, T.D.; Khan, M.K.A.A. Performance Analysis of Machine Learning Algorithms in Intrusion Detection System: A Review. *Procedia Computer Science* **2020**, *171*, 1251–1260, doi:10.1016/j.procs.2020.04.133.